The EMBO Journal Vol.16 No.5 pp.989–997, 1997

1.9 Å crystal structure of interleukin 6: implications for a novel mode of receptor dimerization and signaling

William Somers[1], Mark Stahl and Jasbir S.Seehra

Small Molecule Drug Discovery, Genetics Institute, Inc., 87 Cambridge Park Drive, Cambridge, MA 02140, USA

[1]Corresponding author

Interleukin 6 (IL-6) has many biological activities *in vivo*, and deregulation has been implicated in many disease processes. IL-6, a 185 amino acid polypeptide was refolded, purified and crystallized. The crystals diffracted to beyond 1.9 Å and the structure was solved using single isomorphous replacement. The X-ray structure of IL-6 is composed of a four helix bundle linked by loops and an additional mini-helix. 157 out of 185 residues are well defined in the final structure, with 18 N-terminal and 8 A–B loop amino acids displaying no interpretable electron density. The three-dimensional structure has been used to construct a model of IL-6 interacting with the IL-6 receptor (α-chain) and gp130 (β-chain) that gives new insight into the process of molecular recognition and signaling. Based on this model, we predict a fourth binding site on IL-6, a low affinity IL-6–IL-6 interaction, which may be necessary for the sequential assembly of a functional hexameric IL-6 receptor complex.

Keywords: crystal structure/interleukin 6/receptor/signaling

Introduction

Interleukin 6 (IL-6) is a pleiotropic cytokine with a variety of stimulatory effects on hematopoietic cells and cells of the immune system (Hirano *et al.*, 1986; Wong *et al.*, 1988; Kishimoto *et al.*, 1992). Major cellular targets include B lymphocytes, T lymphocytes, the enhancement of hematopoietic colony formation and the production of acute phase response proteins in the liver (Mackiewicz *et al.*, 1992). IL-6 appears to be a component of the immune system, with knock-out mice exhibiting an impaired IgG and IgA response (Kopf *et al.*, 1994; Ramsay *et al.*, 1994). Of particular interest is the observation of the involvement of IL-6 in bone homeostasis. In Paget's disease and in multiple myeloma patients where significant bone loss occurs, a good correlation has been found with increased IL-6 levels. Interestingly, the level of IL-6 is affected by estrogen in bone marrow-derived stromal cells and causes a decrease in the development of osteoclasts (Girasole *et al.*, 1992), while estrogen loss (by mouse ovariectomy) causes enhanced osteoclast development in *ex vivo* cultures of bone marrow and increased osteoclasts in trabecular bone. Most importantly, osteoclast development was inhibited by the *in vivo* or *in vitro* administration of estrogen or neutralizing IL-6 monoclonal antibodies (Jilka *et al.*, 1992). Mutant mice lacking IL-6 have normal amounts of trabecular bone and ovariectomy does not cause bone loss or a change in the rate of remodeling (Poli *et al.*, 1994). These studies strongly suggest that IL-6 plays an important role in post-menopausal bone loss.

IL-6 belongs to a family which share remarkably similar structural features both for the cytokines and the receptors to which they bind. These similarities also extend to the sequential clustering events leading to signal transduction. The closest members of the family include leukemia inhibitory factor (LIF), cillary neurotrophic factor (CNTF), oncostatin M and IL-11 (Yamasaki *et al.*, 1988; Davis *et al.*, 1991; Gearing *et al.*, 1991; Kishimoto *et al.*, 1992, 1994; Miyajima *et al.*, 1992). IL-6 receptor consists of two polypeptides: the α chain (IL-6r), an 80 kDa transmembrane glycoprotein that binds IL-6 with low affinity, and the β chain (gp130), a 130 kDa transmembrane glycoprotein that binds to the IL-6–IL-6r heterodimer to form the high affinity signal transducing complex (Taga *et al.*, 1989). The IL-6r is a transmembrane protein composed of a cytokine binding type I domain (necessary and sufficient for binding IL-6; Yawata *et al.*, 1993), an Ig-like domain and a short cytosolic domain (Yamasaki *et al.*, 1988) that is not required for signaling (Taga *et al.*, 1989). gp130 is also a transmembrane protein composed of an Ig-like domain, cytokine type I domain, a contactin-like region, a transmembrane domain and a cytosolic domain necessary for signaling, containing a motif known as box1, box2 (Murakami *et al.*, 1991). gp130 is a signal transduction component of not only the IL-6 receptor but also the LIF, CNTF, oncostatin M and the IL-11 receptors (Taga *et al.*, 1992); therefore, the α chain distribution dictates the cellular response (Kishimoto *et al.*, 1992). Signal transduction by IL-6 follows the dimerization of gp130, which activates a bound JAK2 (Argetsinger *et al.*, 1993).

Recently, studies utilizing size exclusion chromatography and equilibrium centrifugation have shown that IL-6 binds to the soluble extracellular domain of IL-6r (sIL-6r) to form a heterodimer (Ward *et al.*, 1994). However, in the presence of the soluble extracellular domain of gp130 (sgp130), a hexameric complex is formed that is composed of IL-6, sIL-6r and sgp130 in a 2:2:2 stoichiometry (Ward *et al.*, 1994). These studies, combined with the evidence from structural, biochemical and mutagenesis studies of the human growth hormone (hGH), human growth hormone receptor (hGHr) and human prolactin receptor (hPRLr) complexes (De Vos *et al.*, 1992; Somers *et al.*, 1994), provide evidence that assembly of the IL-6 signaling complex is an ordered and sequential process.

Analysis of IL-6 site-directed mutagenesis data provides further support for such a structural model. The first class

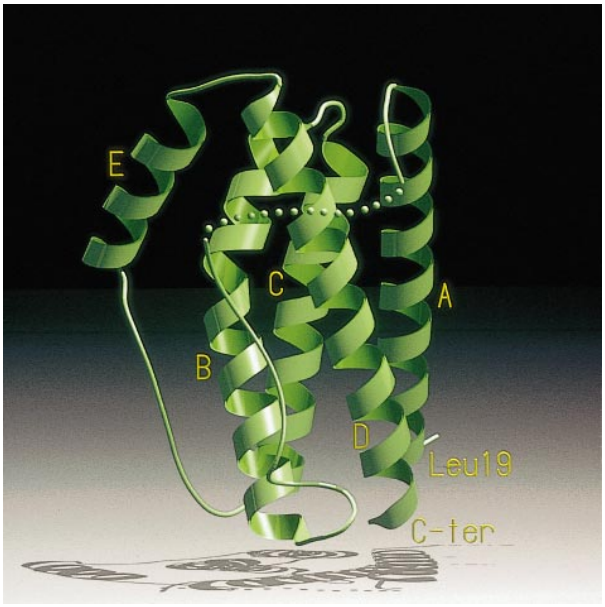

Fig. 1. Ribbon representation of the IL-6 crystal structure. The four main helices are labeled A, B, C and D. The extra helix in the final long loop is labeled E. The missing part of the first cross-over connection is indicated by a dashed line. The figure was created using MOLSCRIPT (Kraulis, 1991) and RAYSHADE.

of IL-6 mutants (site 1) show reduced binding to IL-6r (Savino *et al.*, 1993). Two additional, distinct classes of IL-6 mutants (sites 2 and 3) have been isolated which bind to IL-6r and yet fail to transduce (Brakenhoff *et al.*, 1994; Ehlers *et al.*, 1994). IL-6 with both site 2 and site 3 mutations not only fails to transduce signal but functions as an antagonist in an IL-6-dependent proliferation assay (Brakenhoff *et al.*, 1994). IL-6r point mutants have also been identified which result in normal IL-6 binding but no signal transduction (Yawata *et al.*, 1993). It has been speculated that these mutations are in a region of IL-6r that is involved in low affinity binding to gp130.

We report here the 1.9 Å X-ray structure of human recombinant IL-6 and compare the structure of IL-6 with known structures of other closely related cytokines. The availability of the three-dimensional structure allows a detailed interpretation of previously reported mutagenesis studies and a better understanding of how they affect IL-6r–gp130 binding. A three-dimensional model of the hexameric IL-6 receptor complex is also presented based upon reported mutagenesis studies, biochemical data and the structure of the hGHr complex. Based on our model, we predict a fourth binding site on IL-6, a IL-6–IL-6 interaction, which may be necessary for the sequential assembly of a functional hexameric IL-6 receptor complex.

Results

Protein structure

The crystal structure of IL-6 (Figure 1) is a four helix bundle with a topology that has now been seen for a number of other cytokines in the superfamily described by Bazan (Bazan, 1990, 1991; Sprang and Bazan, 1993). The four helices are arranged so that the helices A and B run in the same direction and C and D in the opposite direction. Linking the helices in this arrangement is made possible by a long loop joining the A and B helices, a short one between B and C and finally a second long connection between C and the fourth main helix D.

Backbone structure

The N-terminal 18 amino acids of IL-6 are not visible in electron density maps and consequently have not been modeled. The first long helix (A) extends from Ser21 to Ala45 and is connected to helix B by a 25 amino acid loop. The first structural feature of the inter-helix connection is a loop formed by a disulfide bond between cysteines 44 and 50. Cys50 is poorly ordered and precedes an eight residue break with no interpretable electron density. This break is followed by Ala61–Glu69 in an extended conformation which presents the hydrophobic side chains of Leu62, Leu64, Phe65 and Met67 into a cleft between helices B and D. Before the start of helix B, the final section of the loop is defined by three structural elements, a type I β turn (Ala68–Asp71), a disulfide (Cys73–Cys83) and a type II β turn (Gln75–Phe78).

Helix B (Glu80–Gln102) has average ϕ,ψ torsion angles of –63.8 and –39.5°. The ϕ,ψ values for Glu93 and Phe94 are –64.5,–25.6° and –76.8,–16.5° respectively, caused by a 38° bend in the direction of the helix axis centered at these residues. This bend results in a break in the α-helical hydrogen bonding pattern, such that Leu92 O is hydrogen-bonded to Val96 N via water 19. The short cross-over connection between helices B and C extends from Asn103 to Ser108 and has higher than average *B*-factors (37.9 $Å^2$).

Helix C (Glu109–Lys129) is followed by the second long cross-over connection. Residues Leu133–Asp140 are in an extended conformation interacting with helix B via the hydrophobic side chains of Leu133, Ile136 and Pro139. Following this there is an additional short helix (E) lying outside the main four helical bundle. The three turns of this helix are formed by amino acids from Pro141 to Gln152.

Residues Gln156–Arg182 form the final D helix. Located at the N-terminus of this helix is the only tryptophan (157) in IL-6. In solution, this tryptophan would be solvent exposed but in the crystal is buried in a hydrophobic pocket made by two symmetry-related molecules. The two C-terminal residues of IL-6, Gln183 and Met184, have higher than average *B*-factors (35.8 $Å^2$) but good electron density.

Side chain contacts

The relative disposition of the four main helices of IL-6 is maintained by a network of hydrophobic interactions in the core of the molecule. These interactions occur in layers of residues down the entire axis of the bundle. The lower end of the core (Figure 1) is capped by a hydrogen bond between the side chains of Lys129 and Ser22 and hydrophobic interactions between Leu84 and Met184. The core residues are Ile25, Ile29, Ile32, Ile36, Leu39, Thr43, Ile87, Leu91, Leu98, Leu101, Phe105, Ala112, Val115, Thr119, Leu122, Leu126, Thr163, Leu167, Phe170, Leu174, Ser177 and Leu181. This core is terminated at the other end by a hydrogen bond between Ser108 and Glu42. Side chains in the core that are capable of forming hydrogen bonds make interactions away from the center.

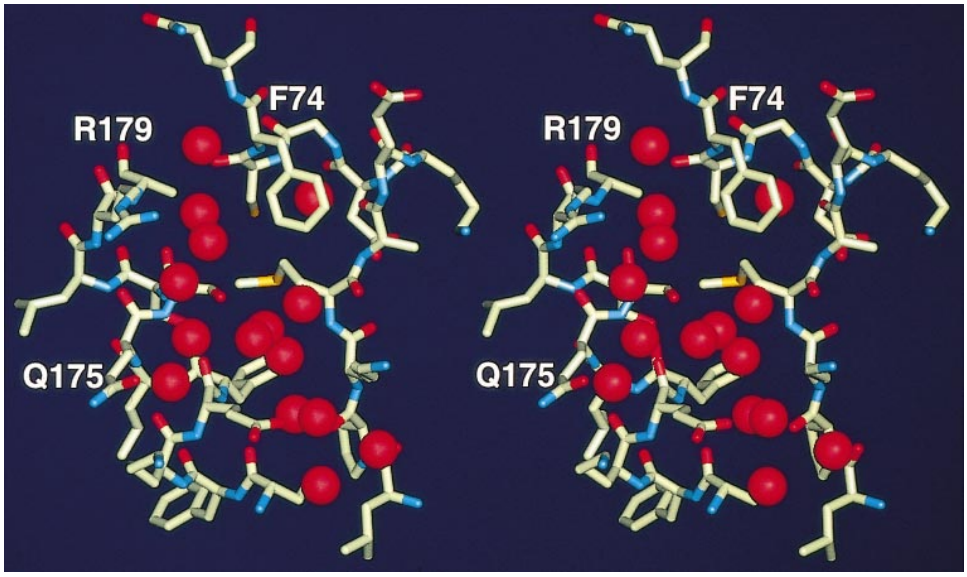

Fig. 2. Stereo view of the water structure in the region between the D helix and the A–B loop of IL-6. The water molecules are shown as red spheres and the protein as a stick representation.

Thr43 Oγ interacts with an ordered water, Thr119 Oγ donates a hydrogen bond to Val115 O, Thr163 Oγ donates a hydrogen bond to Gln159 O and Ser177 Oγ donates to Phe173 O. On the outside of this main hydrophobic core lies a cluster of hydrophobic side chains stabilizing the position of the E mini-helix. This mini-helix presents the side chains of three leucines (147,148,151) towards the hydrophobic side chains of helix B (Val96, Tyr97, Tyr100), helix D (Thr162) and the A–B loop (Leu62).

In contrast to the large number of hydrophobic interactions stabilizing the fold of IL-6, only three hydrogen bonds bridge the main helices. Indeed, helix A has no hydrogen bonds with the other helices. Helices B and C interact via a hydrogen bond between the Oε1 of Glu95 and Nζ of Lys120 (2.5 Å). The only other two hydrogen bonds between helices B and D are formed by Arg104 Nη2 to Asp160 Oδ1 (3.0 Å) and Tyr100 Oη to Gln159 Nε2 (2.8 Å). In addition, there is a considerable network of indirect hydrogen bonds via networks of ordered water molecules (described below).

The crystal structure of IL-6 shows that the side chains of Asp26, Arg30 and Met117 each exist in two discrete conformations. The Asp and Arg residues interact with each other and are next to a crystallographic 2-fold axis. In one state, Arg30 donates a hydrogen bond (2.8 Å) from the Nε to Oδ1 of Asp26 ($\chi1 = -174°$). In the second state, rotation of χ torsion angles (Asp26 $\chi1 = -73°$) breaks this hydrogen bond so the arginine now donates a hydrogen bond to water 34 (2.8 Å) and Asp26 hydrogen bonds to water 55 (2.6 Å). In the first conformation, Arg30 interacts with itself and makes a close contact to Asp26 (1.7 Å) through the crystallographic 2-fold axis so that adjacent molecules require the second conformation.

Trp157 which lies at the N-terminal end of helix D is almost completely solvent exposed aside from contacts (3.5 Å) with the Cε of Met49. Despite being solvent exposed, this tryptophan is highly ordered through its interactions with a symmetry-related molecule and penetrates deep into a hydrophobic pocket created by the side chains of helices A (Tyr31 and Gly35) and C (Ala114, Val115 and Ser118). The solvent accessibility of the tryptophan is consistent with the fluorescence emission spectra with $\varepsilon_{\lambda max}$ ~336 nm (data not shown).

Ordered water

The current model of IL-6 contains 121 ordered water molecules, of which 105 have temperature factors ranging from 15.4 to 50.0 $Å^2$ (16 water molecules have temperature factors >50.0 $Å^2$). There are only nine water molecules in the second shell which do not interact directly with protein. The ordered water molecules are not distributed uniformly over the entire surface of IL-6 but are localized to clefts in the surface. These water molecules form networks of hydrogen bonds that link the helices and loops that stabilize the crystal structure. One water molecule (47) is completely buried between helices B and C and bridges the two helices by forming hydrogen bonds to the carbonyl oxygens of Ala112 (2.8 Å) and Leu98 (3.0 Å).

The highest density of water is found in the region between the C-terminal regions of helix D and the A–B loop (Figure 2). There are 18 water molecules and two sulfates in this region that form a network of hydrogen bonds linking these two secondary structural elements. From modeling studies described later, this region may be involved in binding to the IL-6r.

Small molecule binding

The crystal structure of IL-6 has a single L(+)-tartaric acid molecule bound on a crystallographic 2-fold axis giving a stoichiometry of one tartrate bound to two molecules of IL-6. The binding is mediated by direct hydrogen bonds from Arg182 Nε (2.8 Å) and Nη2 (2.7 Å) to one carboxyl group of tartrate. The same carboxyl atoms hydrogen-bond with Arg179 Nε (2.8 Å) and water 6 (3.0 Å). In addition, the α-OH of tartrate accepts a hydrogen bond from Arg179 Nη2 (3.0 Å) and the β-OH donates a hydrogen bond to the O of Gln175 (2.8 Å). Since the tartrate lies on a crystallographic 2-fold axis,

these interactions are duplicated on the other half of the tartrate from a symmetry-related molecule satisfying almost every possible hydrogen bond.

Structural comparison of IL-6 with G-CSF and hGH

The four helix bundle up–up, down–down topology of the helices seen in the structure of IL-6 was predicted by Bazan (Bazan, 1990, 1991; Sprang and Bazan, 1993) to be a common structural fold for cytokines. Although the members of the superfamily share low homology at the amino acid level, the three-dimensional structures of several cytokines reveal a remarkable similarity. Granulocyte colony-stimulating factor (G-CSF), with 16% amino acid sequence identity, is the closest member of the superfamily for which a three-dimensional structure is available (Bazan, 1991). The structures of human G-CSF (hG-CSF; Hill *et al.*, 1993), canine G-CSF and bovine G-CSF (Lovejoy *et al.*, 1993) have all been determined to high resolution. hG-CSF, with the most ordered residues, has been chosen for a detailed comparison with IL-6. hGH shares only 9% amino acid sequence identity with IL-6. hGH has been examined crystallographically in complex with the extracellular domain of its receptor (De Vos *et al.*, 1992) so that a comparison with IL-6 gives insights into the interaction of IL-6 with its receptor (IL-6r) and gp130.

The superposition of G-CSF (Figure 3) on IL-6 using 88 Cα atoms in the helices gives an agreement of 1.1 Å root-mean-square (r.m.s.) between the two structures. For the more distantly related hGH, the agreement is only 1.4 Å r.m.s. over 83 atoms. This superposition reveals a good agreement in both the inter-helix angles and length of helices in these cytokines. However, a close examination reveals significant differences in several regions. The N-termini of IL-6 and G-CSF are disordered so that the crystal structures of both begin at the start of helix A, whereas the N-terminal residues of hGH are ordered and are involved in receptor binding. Helix A is the same length for all three cytokines but does not superimpose well at the C-terminal end. The largest differences at the C-terminal end of this helix are seen for hGH, which may be influenced by the position of the short loop between helices B and C. Following helix A, the first long loop exhibits considerable conformational variability. The disulfide bonds in G-CSF and IL-6 in this region stabilize a very similar conformation for the A–B loop immediately after helix A. However, immediately following this, IL-6 is disordered while the other cytokines have short helical segments. The final part of the loop has the second conserved disulfide which constrains IL-6 and G-CSF to adopt very similar conformations whereas hGH has a second short helix (Figure 3).

Helix B superimposes well at the N-terminus for all three cytokines. IL-6 and hGH both have kinks in the same position in helix B due to a break in the hydrogen bonding and continue to superimpose well after this point. G-CSF does not have this break and extends for another turn. The short loop that connects helices B and C has a different conformation in each case, while hGH includes a three residue insertion, which allows the loop to extend much closer to helix A.

Helix C superimposes well for all three cytokines except in hGH, where it is four residues shorter at the N-terminus. The long loop following helix C is well ordered in IL-6 but lacks residues present in the other two cytokines. At the end of this loop, IL-6 has a helical segment while G-CSF has a short segment of extended conformation. The final long helix (D) is the same length for each structure but does not superimpose well for hGH, which has 10 additional residues extending beyond the C-termini of the other two cytokines.

Discussion

IL-6 is a member of the four helix bundle cytokine superfamily which share structural similarities and may share common modes of receptor engagement and activation. These similarities enable signaling models to be constructed that account for the available mutagenesis data. The crystal structure of hGH bound to two molecules of hGHr (De Vos *et al.*, 1992) has provided a useful model for the activation of cytokine receptors upon ligand binding. hGH initially binds an hGHr via a high affinity site on the surface of the cytokine. This dimer of one hGH and one hGHr then binds to a second hGHr. The binding site for the second hGHr is made up of a combination of two low affinity sites: one on the surface of hGH and a site in the C-terminal domain of the first bound receptor. This combination of high and low affinity sites on the surface of hGH ensures that the clustering of hGHr molecules, leading to signaling, is an ordered event.

IL-6-mediated signal transduction has been shown to occur through clustering of two gp130 receptors by IL-6 (Murakami *et al.*, 1993) or an agonistic anti-gp130 monoclonal antibody (Wijdenes *et al.*, 1995). IL-6 binds to a single molecule of IL-6r and forms a heterodimer. In an analogous manner to hGH signaling, this heterodimer is capable of binding to gp130 to form a heterotrimer (IL-6, IL-6r and gp130) with 1:1:1 stoichiometry. Since signaling has been demonstrated to occur through clustering of gp130 molecules, an additional binding step is necessary. Indeed, ultracentrifugation experiments with soluble IL-6, IL-6r and gp130 give a hexamer composed of two molecules of each component (Ward *et al.*, 1994), providing support for an additional clustering event. Recently, Paonessa and co-workers (Paonessa *et al.*, 1995) presented a model of such a hexamer which was based on a model of IL-6, the hGHr complex (De Vos *et al.*, 1992) and information from biochemical studies. We present a more detailed model of the signaling complex based on the high resolution structure of IL-6 in Figure 4A. This model can be used to rationalize the mutagenesis studies of IL-6.

The first event in signal transduction is the binding of soluble IL-6 through site 1 to IL-6r, forming a heterodimer. The second event is the binding of this heterodimer to gp130 on the cell surface. This binding event is mediated through site 2 on IL-6 interacting with gp130 as well as contacts between the C-terminal domains of IL-6r and gp130. The third event to take place in IL-6 signaling is the binding of two hetero-trimeric complexes mediated by interactions in sites 3 ($IL\text{-}6_{trimer\ 1}$–$gp130_{\ trimer\ 2}$) and 4 ($IL\text{-}6_{trimer\ 1}$–$IL\text{-}6_{trimer\ 2}$). This model also predicts the possibility of additional interactions between different trimers via the C-terminal halves of the cytokine-binding domains of IL-6r and gp130.

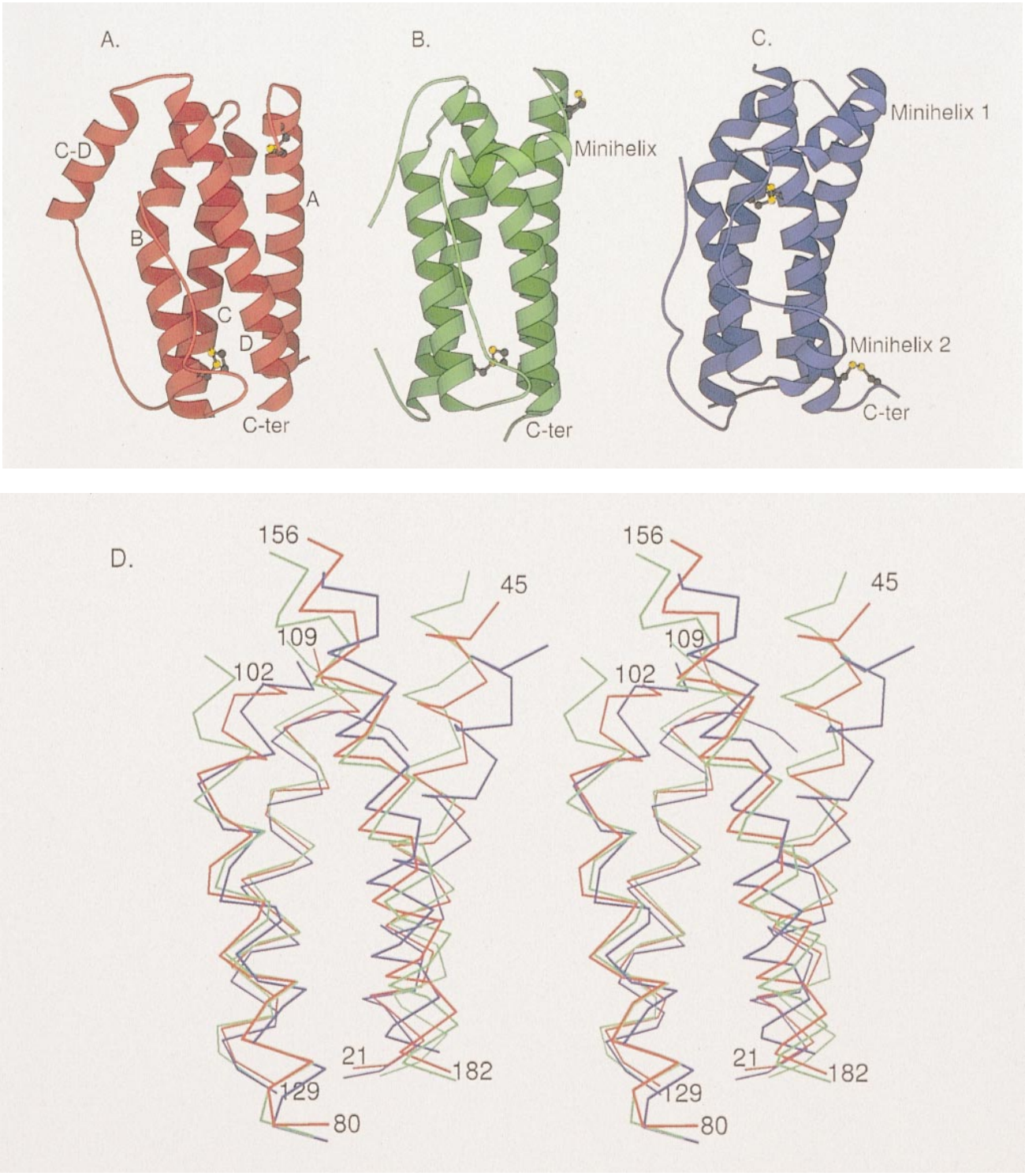

Fig. 3. A comparison of the crystal structures of IL-6 (**A**), hG-CSF (**B**) and hGH (**C**). The disulfide bonds for each cytokine are shown in ball and stick representation. The C-termini are labeled along with main helices and extra helices in the loops. (**D**) A stereo Cα trace of the IL-6 (red) main four helices superimposed on the corresponding sections of hG-CSF (green) and hGH (blue). The figure was produced with MOLSCRIPT (Kraulis, 1991).

Numerous mutagenesis studies have been performed on IL-6 in an effort to define the receptor binding sites (Fiorillo *et al.*, 1992; Fontaine *et al.*, 1993; Savino *et al.*, 1993, 1994b; Ehlers *et al.*, 1994; Hammacher *et al.*, 1994; de Hon *et al.*, 1995; Ehlers *et al.*, 1995). The data from these mutagenesis studies are re-examined in light of the high resolution crystal structure of IL-6 and are represented as space-filling side chains in Figure 4B.

Site 1 mutants discussed by Savino and co-workers (Savino *et al.*, 1993) are consistent with the hexamer model and map to a region on hGH found to be essential for hGHr binding (Cunningham and Wells, 1989). The

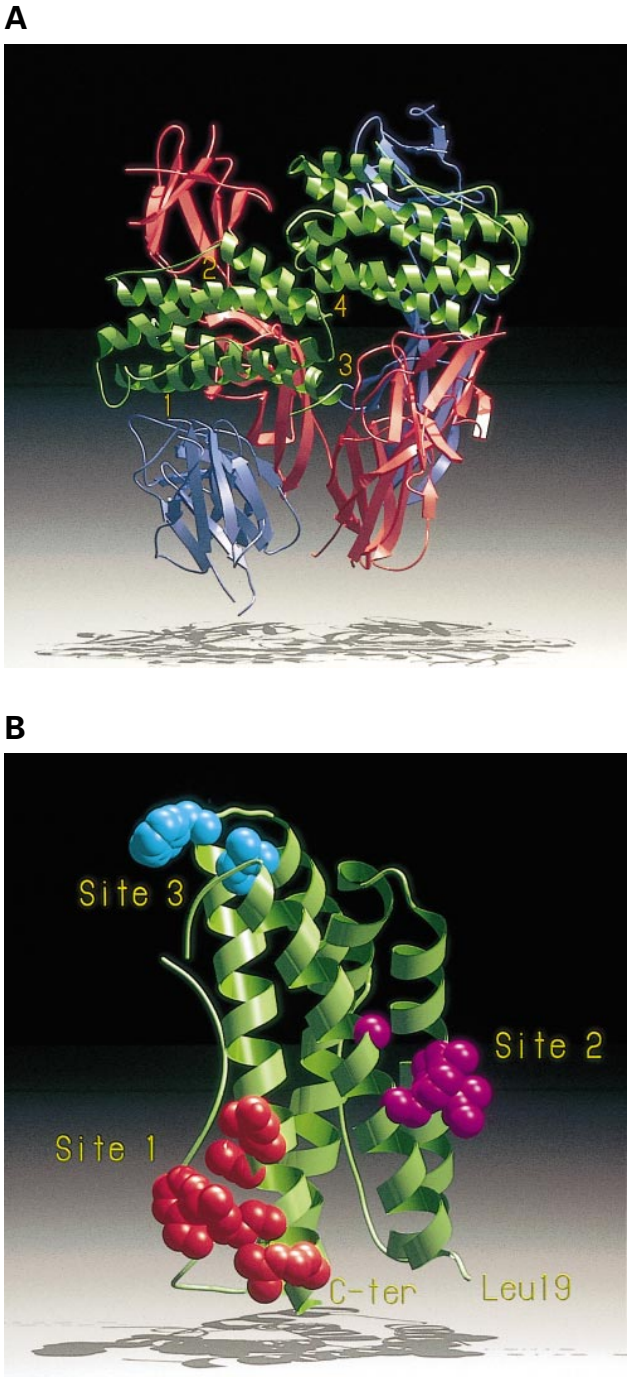

Fig. 4. (**A**) A ribbon representation of the IL-6, IL-6r and gp130 hexamer signaling model. The IL-6 crystal structure is shown in green, IL-6r in blue and gp130 in red. The proposed binding sites are labeled. Site 1 is the site of IL-6–IL-6r interactions. Site 2 is the region where IL-6 interacts with gp130 in the trimer. Site 3 is the site of IL-6–gp130 interactions between trimers. Site 4 is the location of IL-6–IL-6 interactions between trimers. (**B**) A ribbon representation of IL-6 with space-filling atoms of exposed side chains found to alter IL-6r binding (site 1) or gp130 binding (sites 2 or 3) when mutated.

two most important binding determinants on hGHr for hGH were found to be tryptophans 104 and 169 (Clackson and Wells, 1995). These tryptophans are inserted into pockets created by mutationally sensitive hGH residues. After superimposition of IL-6 onto hGH in the receptor complex, it is found that these tryptophans from hGHr

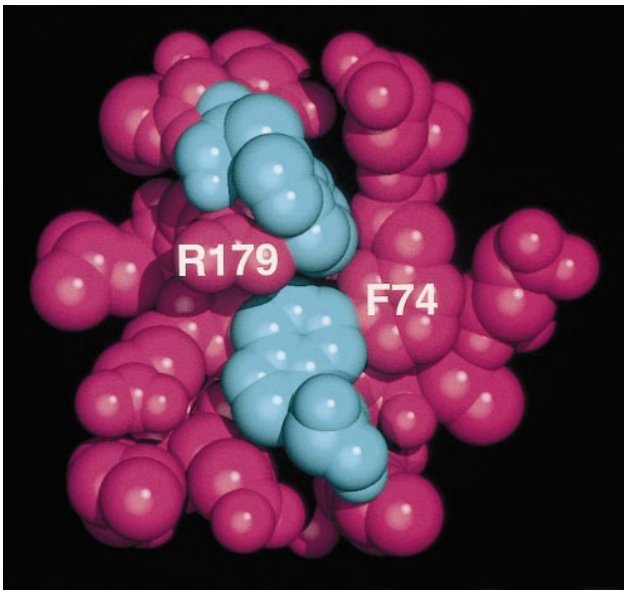

Fig. 5. A van der Waals representation of site 1 on IL-6 (magenta), proposed to be the location of IL-6r binding. In blue are tryptophans 104 and 169 from hGHr positioned by superimposing IL-6 on hGH in the hGHr complex (De Vos *et al.*, 1992). The residues labeled on IL-6 are found to be binding determinants by mutagenesis.

are inserted into a cleft on the surface of IL-6 (Figure 5). A sequence alignment of receptors shows that IL-6r does not have equivalent tryptophans but may use other large or aromatic residues to bind to the surface of IL-6. The importance of this cleft in the surface of IL-6 is demonstrated by the fact that mutants that affect binding of IL-6r all map to this region (Figures 4B and 5). Consistent with this model, a 100-fold decrease in activity is observed upon mutation of Arg179 to Ala (Fontaine *et al.*, 1993). Mutation of Gln175 to Ala results in a 5-fold decrease in activity (Savino *et al.*, 1993). Interestingly, replacement of Ser176 with Arg causes a 4-fold increase in the activity of IL-6 (Savino *et al.*, 1993). The equivalent residue in hGH is Lys172 which forms the pocket that accepts the tryptophan from hGHr. Arg182 (Lutticken *et al.*, 1991) and Phe74 also form the sides of the cleft and are mutationally sensitive (G.Ciliberto, personal communication). Other mutations in this region which affect binding, Ser177, Ala180, Leu178 and Leu181, are all buried and may be affecting activity by altering the local conformation of IL-6. This region is also the location of the highest density of ordered water molecules (Figure 2) which may play a role in binding receptor by adding entropy to the system as they are displaced.

Site 2 mutations, which bind normally to IL-6 but have reduced affinity for binding to the first molecule of gp130 (Savino *et al.*, 1994a,b), are also consistent with the hexamer model. These mutations are localized to a region on helices A and C and consist of Tyr31→Asp, Gly35→Phe, Ser118→Arg and Val121→Asp (Figure 4B). All are exposed and, with the exception of Gly35, close to site 2 used by IL-6 binding to gp130 in the hexamer model. The reduction in activity observed by the mutation of Gly35 to Phe may be due to indirect longer range effects resulting from the insertion of a large hydrophobic side chain.

In addition to the mutations described above, a chimera consisting of human IL-6 with murine residues 43–55 has

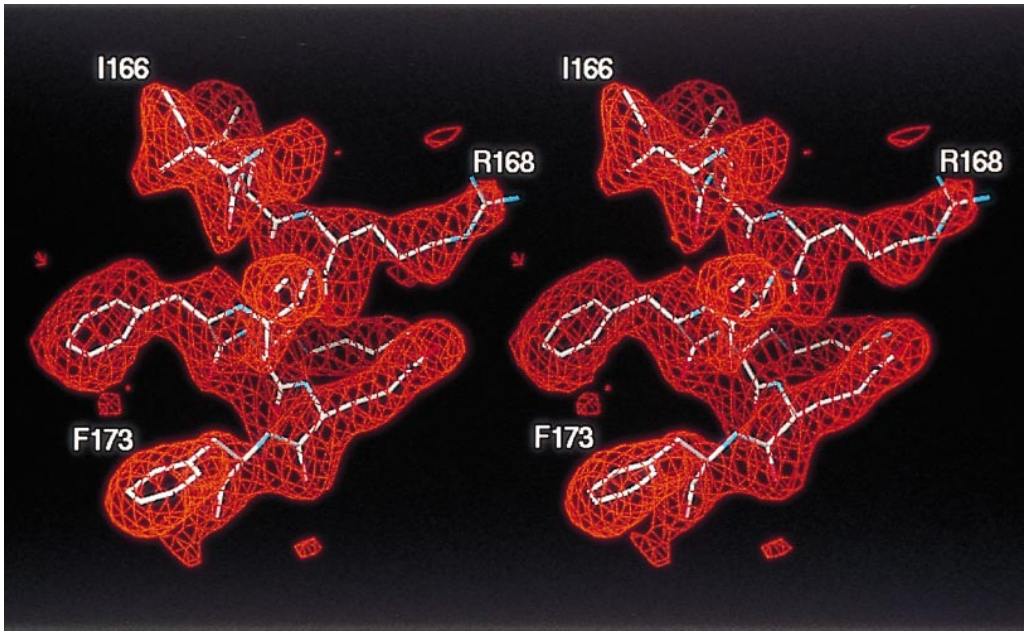

Fig. 6. A stereo plot of a good region of IL-6 2.8 Å electron density phased using single isomorphous replacement with anomalous scattering and solvent flattening.

reduced signalling activity but unaltered affinity for IL-6r (Ehlers *et al.*, 1994). Examination of the hexamer model suggests that this region of IL-6 is important for interaction with the second molecule of gp130 via site 3. Other mutants consistent with site 3 in the hexamer model are located at the N-terminus of helix D. Trp157→Arg and Asp160→Arg (Paonessa *et al.*, 1995) are both exposed and able to interact directly with the second gp130 receptor in this model (Figure 4B). The other residues in this region [Gln159→Glu and Thr162→Pro/Thr162→Asp (Brakenhoff *et al.*, 1994; de Hon *et al.*, 1995)] are both buried and consequently may affect gp130 binding indirectly.

Our model predicts additional interactions between two molecules of IL-6 which stabilize the signaling complex. Based on this model, we predict that the region Glu106–Arg113 on IL-6 would interact with the same residues on an adjacent IL-6 across a local 2-fold axis of rotation. The details of these interactions are currently the subject of further investigation.

The structure of IL-6 has allowed further refinement of the hexameric model presented by Paonessa *et al.* (1995) and has enabled a more detailed understanding of the available mutagenesis data. Since LIF, CNTF, oncostatin M and IL-11 all share gp130 as a common signal transducer and are predicted to have similar four helical structures, it seems likely that a hexameric complex may be a common feature of signal transduction for this family of cytokines.

Materials and methods

Recombinant IL-6 expressed in *Escherichia coli* was refolded (Arcone *et al.*, 1991) and purified with ion exchange and hydrophobic interaction chromatography. Purified IL-6 at 15 mg/ml was crystallized using hanging drop vapor diffusion from 1.8 M ammonium sulfate, 300 mM sodium potassium tartrate, in 100 mM pH 6.3 sodium citrate buffer. The largest crystals measured 0.6×0.4×0.2 mm and took up to 2 months to grow at 4°C.

Table I. IL-6 data reduction and phasing statistics for a native crystal and single derivative

	Native	Derivative
Resolution	10.0–1.9	10.0–2.4
Number of observations[a]	100 519	31 588
Number of unique reflections	14 002	7203
Completeness (%)	97.6	99.1
Reflections with I>3σI (%)	93.0	95.1
R-merge[b]	0.031	0.029
Fractional isomorphous difference[c]		0.264
Cullis *R*-factor[d] acentric/centric		0.57,0.53
Phasing power[e] acentric/centric		2.22,1.84
Figure of merit		0.57

[a]Number of observations after pairing partial reflections in adjacent images.
[b]*R*-merge = $\Sigma|I_j - \langle I \rangle|/\Sigma I_j$ where I_j is the intensity of a measured observation and $\langle I \rangle$ is the average of all symmetry equivalents of that observation.
[c]Fractional isomorphous difference = $\Sigma||F_{PH}|-|F_P||/\Sigma|F_P|$ where F_P is the native structure factor amplitude and F_{PH} that of the derivative.
[d]Cullis *R*-factor is the lack of closure residual/isomorphous difference.
[e]Phasing power = r.m.s. F_H/lack of closure, where F_H is the calculated heavy atom contribution.

Intensity data were collected using a Rigaku R-Axis II image plate on a RU-200 X-ray generator running at 5 kW with mirror focusing optics. Examination of the symmetry of reduced rotation data and the pattern of systematic absences on rotation images clearly indicated crystals were of space group P3121 or P3221 with cell parameters a = 49.7 Å and c = 122.0 Å. All high resolution data sets were collected at –168°C on crystals soaked in 20% glycerol as a cryoprotectant. These crystals were found to be highly ordered, diffracting to beyond 1.9 Å resolution. The image plate data were processed with DENZO (Otwinowski, 1993) then scaled with ROTAVATA and AGROVATA (Collaborative Computing Project number 4, 1994) giving the statistics listed in Table I. The structure was solved using single isomorphous replacement with anomalous scattering (SIRAS) prepared by soaking the crystal in 1 mM potassium tetrachloroaurate(III) for 24 h at 4°C. The gold heavy atom derivative gave a single site located using isomorphous difference Pattersons and then confirmed with a clear signal in the anomalous difference Patterson. Refinement of the heavy atom occupancy, position and isotropic thermal parameters followed by calculation of phases was

performed using MLPHARE (Otwinowski, 1991) as part of the CCP4 suite of programs (Collaborative Computing Project number 4, 1994). The phasing statistics reported by MLPHARE are shown in Table I.

Space group ambiguity was resolved by examining 2.8 Å electron density maps phased including the anomalous data. Space group P3121 gave a clear protein–solvent boundary with density that corresponded well with the secondary structural elements of the related cytokine hG-CSF (Hill *et al.*, 1993). The related space group P3221 gave no recognizable protein features. Electron density was improved further with solvent flattening (Wang, 1985) giving high quality 2.8 Å maps (Figure 6) that were used to build an initial model using QUANTA (Biosym/Molecular Simulations, San Diego, CA) and O (Jones *et al.*, 1991). The model and electron density maps were improved with repeated rounds of least-squares refinement using PROLSQ (Hendrickson, 1985), SIGMAA weighting (Read, 1986) and phase combination at 2.4 Å. Prior to refinement of the model, 5% of the reflections were removed to monitor the free *R*-value (Brunger, 1992). In the final 1.9 Å data set collected from a single crystal, these same free *R*-value reflections were maintained so that at the end of refinement these reflections represent a reliable, unbiased indication of the quality of the model. Conventional least-squares refinement with PROLSQ, simulated annealing in XPLOR (Brunger *et al.*, 1987) and, finally, maximum likelihood refinement in REFMAC (Collaborative Computing Project number 4, 1994) were all used to generate the IL-6 model. The final model has an *R*-value of 21.3% for all data in the range 8.0–1.9 Å and a free *R*-value of 27.7% calculated without bulk solvent correction in the program REFMAC. The r.m.s. deviation of the model from ideal geometry reported by REFMAC is 0.017 Å for bond lengths, 0.026 Å for angle distances and the r.m.s. difference in the thermal parameters is 1.5 $Å^2$ between bonded main chain atoms and 3.3 $Å^2$ for side chain atoms. The average *B*-factor for main chain atoms is 24.8 $Å^2$ and for side chains is 28.4 $Å^2$. The Ramachandran plot calculated with PROCHECK (Laskowski *et al.*, 1993) has no residues with backbone torsion angles in disallowed regions and 95.2% in the most favored regions.

The final model consists of 157 residues (1414 atoms) with 121 ordered water molecules, 3.5 sulfates and 0.5 tartrates. In the final electron density maps, residues 1–18, 52–60 and side chains Asn61, Asn63, Glu81, Lys131 and Asn132 are disordered and have not been modeled.

Acknowledgements

We thank E.DiBlasio-Smith and J.McCoy for IL-6 expression plasmids, N.Schauer for fermentation, E.Nickbarg for mass spectroscopy analysis, D.Cumming for graphics assistance and J.Knopf for valuable discussions.

References

Arcone,R., Pucci,P., Zappacosta,F., Fontaine,V., Malorni,A., Marino,G. and Ciliberto,G. (1991) Single-step purification and structural characterization of human interleukin-6 produced in *Escherichia coli* from a T7 RNA polymerase expression vector. *Eur. J. Biochem.*, **198**, 541–547.

Argetsinger,L.S., Cambell,G.S., Yang,X., Witthuhn,B.A., Silvennoinen,O., Ihle,J.N. and Carter-Su,C. (1993) Identification of JAK2 as a growth hormone receptor-associated tyrosine kinase. *Cell*, **74**, 237–244.

Bazan,J.F. (1990) Haemopoietic receptors and helical cytokines. *Immunol. Today*, **11**, 350–354.

Bazan,J.F. (1991) Neuropoietic cytokines in the hematopoietic fold. *Neuron*, **7**, 197–208.

Brakenhoff,J.P.J., de Hon,F.D., Fontaine,V., ten Boekel,E., Schooltink,H., Rose-John,S., Heinrich,P.C., Content,J. and Aarden,L.A. (1994) Development of a human interleukin-6 receptor antagonist. *J. Biol. Chem.*, **269**, 86–93.

Brunger,A.T. (1992) The free *R* value: a novel statistical quantity for assessing the accuracy of crystal structures. *Nature*, **355**, 472–474.

Brunger,A.T., Kuriyan,J. and Karplus,M. (1987) Crystallographic *R* factor refinement by molecular dynamics. *Science*, **235**, 458–460.

Clackson,T. and Wells,J.A. (1995) A hot spot of binding energy in a hormone–receptor interface. *Science*, **267**, 383–386.

Collaborative Computing Project number 4 (1994) The CCP4 suite: programs for protein crystallography. *Acta Crystallogr.*, **D50**, 760–767.

Cunningham,B.C. and Wells,J.A. (1989) High-resolution epitope mapping of hGH–receptor interactions by alanine-scanning mutagenesis. *Science*, **244**, 1081–1085.

Davis,S., Aldrich,T.H., Valenzuela,D.M., Wong,V., Furth,M.E., Squinto,S.P. and Yancopoulos,G.D. (1991) The receptor for ciliary neurotrophic factor. *Science*, **253**, 59–63.

de Hon,F.D. *et al.* (1995) Functional distinction of two regions of human interleukin 6 important for signal transduction via gp130. *Cytokine*, **7**, 398–407.

De Vos,A.M., Ultsch,M. and Kossiakoff,A.A. (1992) Human growth hormone and extracellular domain of its receptor: crystal structure of the complex. *Science*, **255**, 306–312.

Ehlers,M., Grotzinger,J., de Hon,F.D., Mullberg,J., Brakenhoff,J.P.J., Liu,J., Wollmer,A. and Rose-John,S. (1994) Identification of two novel regions of human IL-6 responsible for receptor binding and signal transduction. *J. Immunol.*, **153**, 1744–1753.

Ehlers,M. *et al.* (1995) Combining two mutations of human interleukin-6 that affect gp130 activation results in a potent interleukin-6 receptor antagonist on human myeloma cells. *J. Biol. Chem.*, **270**, 8158–8163.

Fiorillo,M.T., Cabibbo,A., Iacopetti,P., Fattori,E. and Ciliberto,G. (1992) Analysis of human/mouse interleukin-6 hybrid proteins: both amino and carboxy termini of human interleukin-6 are required for *in vitro* receptor binding. *Eur. J. Immunol.*, **22**, 2609–2615.

Fontaine,V., Savino,R., Arcone,R., De Wit,L., Brackenhoff,J.P.J., Content,J. and Ciliberto,G. (1993) Involvement of the Arg179 in the active site of human IL-6. *Eur. J. Biochem.*, **211**, 749–755.

Gearing,D.P., Thut,C.J., VandenBos,T., Gimpel,S.D., Delaney,P.B., King,J., Price,V., Cosman,D. and Beckmann,M.P. (1991) Leukema inhibitory factor receptor is structurally related to the IL-6 signal transducer, gp130. *EMBO J.*, **10**, 2839–2848.

Girasole,G., Jilka,R.L., Passeri,G., Boswell,S., Boder,G., Williams,D.C. and Manolagas,S.C. (1992) 17β-estradiol inhibits interleukin-6 production by bone marrow-derived stromal cells and osteoblasts *in vitro*: a potential mechanism for the antiosteoporotic effect of estrogens. *J. Clin. Invest.*, **89**, 883–891.

Hammacher,A., Ward,L.D., Weinstock,J., Treutlein,H., Yasukawa,K. and Simpson,R.J. (1994) Structure–function analysis of human IL-6: identification of two distinct regions that are important for receptor binding. *Protein Sci.*, **3**, 2280–2293.

Hendrickson,W.A. (1985) Stereochemically restrained refinement of macromolecular structures. *Methods Enzymol.*, **115**, 252–270.

Hill,C.P., Osslund,T.D. and Eisenberg,D. (1993) The structure of granulocyte-colony-stimulating factor and its relationship to other growth factors. *Proc. Natl Acad. Sci. USA*, **90**, 5167–5171.

Hirano,T. *et al.* (1986) Complementary DNA for a novel human interleukin (BSF-2) that induces lymphocytes to produce immunoglobulin. *Nature*, **324**, 73.

Jilka,R.L., Hangoc,G., Girasole,G., Passeri,G., Williams,D.C., Abrams,J.S., Boyce,B., Broxmeyer,H. and Manolagas,S.C. (1992) Increased osteoclast development after estrogen loss: mediation by interleukin-6. *Science*, **257**, 88–91.

Jones,T.A., Zou,J.Y., Cowan,S.W. and Kjeldgaard,M. (1991) Improved methods for building models in electron density maps and location of errors in these models. *Acta Crystallogr.*, **A47**, 110–119.

Kishimoto,T., Akira,S. and Taga,T. (1992) Interleukin-6 and its receptor: a paradigm for cytokines. *Science*, **258**, 593–597.

Kishimoto,T., Taga,T. and Akira,S. (1994) Cytokine signal transduction. *Cell*, **76**, 1–20.

Kopf,M., Baumann,H., Freer,G., Freudenberg,M., Lamers,M., Kishimoto,T., Zinkernagel,R., Bluethmann,H. and Kohler,G. (1994) Impaired immune and acute-phase responses in interleukin-6-deficient mice. *Nature*, **368**, 339–342.

Kraulis,P.J. (1991) MOLSCRIPT: a program to produce both detailed and schematic plots of protein structures. *J. Appl. Crystallogr.*, **24**, 946–950.

Laskowski,R.A., MacArthur,M.W., Moss,D.S. and Thornton,J.M. (1993) PROCHECK: a program to check the stereochemical quality of protein structures. *J. Appl. Crystallogr.*, **26**, 283–291.

Lovejoy,B., Cascio,D. and Eisenberg,D. (1993) Crystal structure of canine and bovine granulocyte-colony stimulating factor (G-CSF). *J. Mol. Biol.*, **234**, 640–653.

Lutticken,C., Kruttgen,A., Moller,C., Heinrich,P.C. and Rose-John,S. (1991) Evidence for the importance of a positive charge and an alpha-helical structure of the C-terminus for the biological activity of human IL-6. *FEBS Lett.*, **282**, 265–267.

Mackiewicz,A.H., Schooltink,P.C., Heinrich,P.C. and Rose-John,S. (1992) The complex of soluble human interleukin-6 receptor/interleukin-6 up-regulates expression of acute phase proteins. *J. Immunol.*, **149**, 2021–2027.

Miyajima,A., Kitamura,T., Harada,N., Yokota,T. and Arai,K. (1992) Cytokine receptors and signal transduction. *Annu. Rev. Immunol.*, **10**, 295–331.

Murakami,M., Narazaki,M., Hibi,M., Yawata,H., Yasukawa,K., Hamaguchi,M., Taga,T. and Kishimoto,T. (1991) Critical cytoplasmic region of the interleukin 6 signal transducer gp130 is conserved in the cytokine receptor family. *Proc. Natl Acad. Sci. USA*, **88**, 11349–11353.

Murakami,M., Hibi,M., Nakagawa,N., Nakagawa,T., Yasukawa,K., Yamanishi,K., Taga,T. and Kishimoto,T. (1993) IL-6-induced homodimerization of gp130 and associated activation of a tyrosine kinase. *Science*, **260**, 1808–1810.

Otwinowski,Z. (1991) Maximum likelihood refinement of heavy atom parameters. In Wolf,W., Evans,P.R. and Leslie,A.G.W. (eds), *Isomorphous Replacement and Anomalous Scattering: Proceedings of the CCP4 Study Weekend*, pp. 23–38.

Otwinowski,Z. (1993) Oscillation data reduction program. In Sawyer,L., Isaacs,N. and Bailey,S. (eds), *Data Collection and Processing: Proceedings of the CCP4 Study Weekend.*

Paonessa,G., Graziani,R., De Serio,A., Savino,R., Ciapponi,L., Lahm,A., Salvati,A.L., Toniatti,C. and Ciliberto,G. (1995) Two distinct and independent sites on IL-6 trigger gp130 dimer formation and signalling. *EMBO J.*, **14**, 1942–1951.

Poli,V., Balena,R., Fattori,E., Markatos,A., Yamamoto,M., Tanaka,H., Ciliberto,G., Rodan,G.A. and Costantini,F. (1994) Interleukin-6 deficient mice are protected from bone loss caused by estrogen depletion. *EMBO J.*, **13**, 1189–1196.

Ramsay,A.J., Husband,A.J., Ramshaw,I.A., Bao,S., Matthaei,K.I., Koehler,G. and Kopf,M. (1994) The role of interleukin-6 in mucosal IgA antibody responses *in vivo*. *Science*, **264**, 561–563.

Read,R.J. (1986) Improved Fourier coefficients for maps using phases from partial structures with errors. *Acta Crystallogr.*, **A42**, 140–149.

Savino,R., Lahm,A., Giorgio,M., Cabibbo,A., Tramontano,A. and Ciliberto,G. (1993) Saturation mutagenesis of the human interleukin 6 receptor binding site: implications for its three dimensional structure. *Proc. Natl Acad. Sci. USA*, **90**, 4067–4071.

Savino,R., Ciapponi,L., Lahm,A,. Demartis,A., Cabibbo,A., Toniatti,C., Delmastro,P., Altamura,S. and Ciliberto,G. (1994a) Rational design of a receptor super-antagonist of human interleukin-6. *EMBO J.*, **13**, 5863–5870.

Savino,R., Lahm,A., Salvati,A.L., Ciapponi,L., Sporeno,E., Altamura,S., Paonessa,G., Toniatti,C. and Ciliberto,G. (1994b) Generation of interleukin-6 receptor antagonists by molecular-modeling guided mutagenesis of residues important for gp130 activation. *EMBO J.*, **13**, 1357–1367.

Somers,W., Ultsch,M., De Vos,A.M. and Kossiakoff,A.A. (1994) The X-ray structure of a growth hormone–prolactin receptor complex. *Nature*, **372**, 478–481.

Sprang,S.R. and Bazan,J.F. (1993) Cytokine structural taxonomy and mechanisms of receptor engagement. *Curr. Opin. Struct. Biol.*, **3**, 815–827.

Taga,T., Hibi,M., Hirata,Y., Yamasaki,K., Yasukawa,K., Matsuda,T., Hirano,T. and Kishimoto,T. (1989) Interleukin-6 triggers the association of its receptor with a possible signal transducer, gp130. *Cell*, **58**, 573–581.

Taga,T. *et al.* (1992) Functional inhibition of hematopoietic and neurotrophic cytokines by blocking the interleukin 6 signal transducer gp130. *Proc. Natl Acad. Sci. USA*, **89**, 10998–11001.

Wang,B.C. (1985) Resolution of phase ambiguity in macromolecular crystallography. *Methods Enzymol.*, **115**, 90–112.

Ward,L.D., Howlett,G.J., Discolo,G., Yasukawa,K., Hammacher,A., Moritz,R.L. and Simpson,R.J. (1994) High affinity interleukin-6 receptor is a hexameric complex consisting of two molecules each of interleukin-6, interleukin-6 receptor, and gp-130. *J. Biol. Chem.*, **269**, 23286–23289.

Wijdenes,J., Heinrich,P.C., Muller-Newen,G., Roche,C., Gu,Z.J., Clement,C. and Klein,B. (1995) Interleukin-6 signal transducer gp130 has specific binding sites for different cytokines as determined by antagonistic and agonistic anti-gp130 monoclonal antibodies. *Eur. J. Immunol.*, **25**, 3474–3481.

Wong,G.G., Witek-Giannotti,J.S., Temple,P.A., Kriz,R., Ferenz,C., Hewick,R.M., Clark,S.C., Ikebuchi,K. and Ogawa,M. (1988) Stimulation of murine hemopoietic colony formation by human IL-6. *J. Immunol.*, **140**, 3040–3044.

Yamasaki,K., Taga,T., Hirata,Y., Yawata,H., Kawanishi,Y., Seed,B., Taniguchi,T., Hirano,T. and Kishimoto,T. (1988) Cloning and expression of the human interleukin-6 (BSF-2/IFNβ 2) receptor. *Science*, **241**, 825–828.

Yawata,H., Yasukawa,K., Natsuka,S., Murakami,M., Yamasaki,K., Hibi,M., Taga,T. and Kishimoto,T. (1993) Structure–function analysis of human IL-6 receptor: dissociation of amino acid residues required for IL-6-binding and for IL-6 signal transduction through gp130. *EMBO J.*, **12**, 1705–1712.

Received on August 26, 1996; revised on October 14, 1996